British Journal of Pharmacology (2003) 139, 919–926 © 2003 Nature Publishing Group All rights reserved 0007–1188/03 $25.00
www.nature.com/bjp

Modulation of ATP-induced currents by zinc in acutely isolated hypothalamic neurons of the rat

[1,2]Vladimir S. Vorobjev, [1,2]Irina N. Sharonova, *,[1]Olga A. Sergeeva & [1]Helmut L. Haas

[1]Department of Neurophysiology, Heinrich-Heine-University, Duesseldorf, Germany

1 Whole-cell patch-clamp and fast perfusion were used to study the effects of zinc on adenosine 5′-triphosphate (ATP)-induced responses of histaminergic neurons.

2 At 10–30 μM ATP, Zn^{2+} had biphasic effects on ATP responses. Zn^{2+} at 3–100 μM increased the ATP-induced currents, but inhibited them at higher concentrations.

3 At 300 μM ATP, Zn^{2+} predominantly but incompletely inhibited the currents.

4 At 5 and 50 μM, Zn^{2+} shifted to the left the concentration–response curve for ATP-induced currents, without changing the maximal response. At 1 mM, Zn^{2+} inhibited ATP-induced currents in a noncompetitive way, reducing the maximal response by 58%.

5 Zn^{2+} increased the decay time of ATP-evoked currents nine fold with an EC_{50} of 63 μM. Upon removal of high concentrations of Zn^{2+}, there was a rapid increase of the current followed by a slow decline towards the response amplitude seen with ATP alone. The appearance of a tail current is consistent with a Zn^{2+}-induced increase of ATP affinity and an inhibition of its efficacy.

6 Thus, Zn^{2+} acts as a bidirectional modulator of ATP receptor channels in tuberomamillary neurons, which possess functional $P2X_2$ receptors. The data are consistent with the existence of two distinct modulatory sites on the P2X receptor, which can be occupied by Zn^{2+}.

7 Our data suggest that zinc-induced potentiation of ATP-mediated currents is caused by the slowing of ATP dissociation from the receptor, while inhibition of ATP-induced currents is related to the suppression of ATP receptor gating.

British Journal of Pharmacology (2003) **139,** 919–926, advance online publication, 2 June 2003; doi:10.1038/sj.bjp.0705321

Keywords: ATP; P2X; zinc; histamine; tuberomamillary

Abbreviations: ATP, adenosine 5′-triphosphate; EC_{50}, the ligand concentration producing a half-maximal response; EGTA, *O*,*O*′-bis(2-aminomethyl)ethyleneglycol-*N*,*N*,*N*′,*N*′-tetraacetic acid; HEPES, *N*-2-hydroxyethylpiperazine-*N*′-2-ethanesulfonic acid; IC_{50}, 50% inhibitory concentration; TM, tuberomamillary

Introduction

Adenosine 5′-triphosphate (ATP) acts as a transmitter or cotransmitter in the central and peripheral nervous systems (for a review, see Ralevic & Burnstock, 1998; Norenberg & Illes, 2000; Khakh, 2001). ATP released from presynaptic terminals can cause a fast excitatory postsynaptic potential in neurons (Edwards *et al*., 1992; Evans *et al*., 1992; Galligan & Bertrand, 1994). Fast responses to ATP are mediated by P2X receptors comprising a family of at least seven P2X subtypes ($P2X_{1-7}$) (Brake & Julius, 1996; North & Surprenant, 2000; Khakh, 2001). All P2X receptors are cation-selective channels with almost equal permeability to Na^+ and K^+ and significant permeability to Ca^{2+} (Evans *et al*., 1996; Koshimizu *et al*., 2000).

Neurons in the rat hypothalamus express mRNA encoding the P2X2, P2X4 and P2X6 subunits (Collo *et al*., 1996; Xiang *et al*., 1998; Kanjhan *et al*., 1999). Furukawa *et al*. (1994) and Sorimachi *et al*. (2001) have reported ATP-activated currents in the neurons of hypothalamic tuberomamillary (TM) and ventromedial nucleus. The pharmacological properties of ATP-mediated responses in TM neurons were consistent with the activation of homomeric $P2X_2$ receptors; however, the presence of heteromeric $P2X_{2/5}$ receptors could not be excluded (Vorobjev *et al*., 2003). In order to further characterize P2X receptors in TM neurons, we have now analyzed the modulation of ATP responses by zinc. The interaction of Zn^{2+} with P2X receptors depends on their subunit composition. Whereas Zn^{2+} inhibits the activity of homomeric $P2X_1$ and $P2X_7$ receptors (Virginio *et al*., 1997; Wildman *et al*., 2002), the activity of $P2X_2$, $P2X_4$ and heteromeric $P2X_4/P2X_6$ receptors is potentiated by Zn^{2+} (Brake & Julius, 1996; Soto *et al*., 1996; Nakazawa *et al*., 1997; Wildman *et al*., 1998; Xiong *et al*., 1999). A biphasic effect of zinc on $P2X_2$, $P2X_4$ and $P2X_{2/6}$ receptors has also been described (Wildman *et al*., 1998; Acuna-Castillo *et al*., 2000; King *et al*., 2000).

Zinc is stored in presynaptic terminals and released upon nerve stimulation (for a review, see Smart *et al*., 1994; Frederickson & Bush, 2001). The effect of zinc on P2X receptors varies in different tissues: it potentiates ATP-induced currents in, for example, spinal cord neurons (Cloues *et al*., 1993), but inhibits ATP-activated currents in bullfrog dorsal

*Author for correspondence at: Heinrich-Heine-Universität, Physiology II, POB 101007, D-40001 Düsseldorf, Germany;
E-mail: olga.sergeeva@uni-duesseldorf.de
[2]Current address: Brain Research Institute, Russian Academy of Medical Sciences, Moscow, Russia.

root ganglion neurons (Li *et al*., 1997). A bidirectional modulation of ATP currents by Zn^{2+} was described in rat vagus neurons (Ueno *et al*., 2001). The effect of Zn^{2+} on native P2X receptors in central neurons has not been studied. We explore now the modulation of ATP-activated currents by zinc in freshly dissociated histaminergic TM neurons using patch-clamp recording techniques.

Methods

Animals and cell preparation

Housing of rats and all procedures were carried out in accordance with the Animal Protection Law of the Federal Republic of Germany. All efforts were made to minimize animal suffering or discomfort and to reduce the number of animals used. After swift decapitation and removal of the brain from the skulls of 18–25-day-old male Wistar rats, 450 μm thick transverse slices containing the TM region were cut and incubated for 1–6 h in a solution containing (mM): 124 NaCl, 3 KCl, 2 $CaCl_2$, 2 $MgCl_2$, 1.28 NaH_2PO_4, 26 $NaHCO_3$, 10 glucose, phenol red 0.01%, bubbled with carbogen (pH 7.4). For preparation of isolated cells, the TM nucleus was dissected from the slice and incubated with papain in crude form (1 mg ml^{-1}) for 40 min at 37°C. After rinsing with enzyme-free solution, the tissue was placed in a small volume of recording solution with the following composition (in mM): 150 NaCl, 3 KCl, 2.5 $CaCl_2$, 1.5 $MgCl_2$, 10 *N*-2-hydroxyethyl-piperazine-*N*′-2-ethanesulfonic acid (HEPES), 10 glucose, pH adjusted to 7.4 with NaOH. Cells were separated by gentle pipetting. Cell suspensions were transferred to the recording chamber and TM neurons were visually identified based on their large cell bodies (20–35 μm) (see Vorobjev *et al*., 2003).

Whole-cell, patch-clamp recording

Voltage-clamp recording was obtained using the whole-cell configuration of the patch-clamp technique. Patch-clamp micropipettes were pulled out from filament-containing thick-wall borosilicate glass tubes using a two-stage puller and had a resistance between 2 and 4 MΩ. The electrodes were filled with a recording solution of the following composition (in mM): 140 $CsCH_3SO_3$; 1 $CaCl_2$; 3 $MgCl_2$; 10 HEPES; 10 *O*,*O*′-bis(2-aminomethyl)ethyleneglycol-*N*,*N*,*N*′,*N*′-tetraacetic acid (EGTA) (pH adjusted to 7.3 with CsOH). The cells were voltage-clamped by an EPC-7 amplifier (HEKA, Germany). Currents were filtered at 2 kHz, sampled at 4 kHz and stored on a hard disk using TIDA acquisition software (HEKA). Recordings were made at a membrane potential of −60 mV at room temperature (22°C). Current amplitudes were always measured at the peak during the application.

Drug application

ATP and $ZnCl_2$ were dissolved in the bath solution and applied using a fast perfusion technique (Vorobjev *et al*., 1996; Sharonova *et al*., 2000). After establishing whole-cell recording, the cell was lifted into the application system, where it was perfused with a control bath solution. All solutions flowed continuously, and lateral movements of the application system exposed a cell either to control solution or to agonist solution. The flow through each tube was gravity-driven. ATP was usually applied for periods of 1 s, at 2 min intervals. For the study of dose–response curves, the intervals between ATP applications were increased up to 4 min at 1–3 mM ATP, to prevent the run-down of ATP responses. The exchange time for the perfusion fluids was estimated by single exponential fitting of the decay time of the current induced by application of 100 μM kainate. In experiments aiming to measure the rate of deactivation of ATP current, it was typically 35 ms.

Data analysis

Agonist concentration–response curves were fit by the least-squares method to

$$I = I_{max}/(1 + (EC_{50}/[ATP])^{h}) \quad (1)$$

where I is the amplitude of ionic current induced by the agonist concentration [ATP], I_{max} is the maximal response, h is the Hill coefficient and EC_{50} is the concentration for which a half-maximal response is induced. The concentration dependence of modulatory effects of zinc and other metal ions upon the current induced by a constant ATP concentration was analyzed with the following equation:

$$I = (1 + I_{max}/(1 + (EC_{50}/[ligand])^{hp}))(c + (1 - c)/(1 + [ligand]/IC_{50})^{hb}) \quad (2)$$

where I_{max} is the relative maximal increase of a response elicited by the ligand. EC_{50} and IC_{50} are the ligand concentrations producing a half-maximal potentiation and a half-maximal inhibition, respectively, *hp* and *hb* are the Hill slopes, [ligand] is ligand concentration and c is the unblocked part of the responses. Data values are presented as mean ± s.e.m.

ATP forms complexes with divalent cations, resulting in a decrease in concentrations of free ATP and metal ions. ATP chelation was estimated using previously reported binding constants of corresponding complexes: $pK_{Ca} = 3.91$, $pK_{Mg} = 4.29$, $pK_{Zn} = 5.16$ (Sigel, 1987). The system of four equations: three equations for equilibrium of each divalent metal: $K_{Mg} = ([\text{total Mg}] - [Mg^{2+}])/([Mg^{2+}]*[ATP^{4-}])$; $K_{Ca} = ([\text{total Ca}] - [Ca^{2+}])/([Ca^{2+}]*[ATP^{4-}])$; $K_{Zn} = ([\text{total Zn}] - [Zn^{2+}])/([Zn^{2+}]*[ATP^{4-}])$ and the equation for ion balance $[\text{total Mg}] - [Mg^{2+}] + [\text{total Ca}] - [Ca^{2+}] + [\text{total Zn}] - [Zn^{2+}] = [\text{total ATP}] - [ATP^{4-}]$) was solved. From four sets of roots, the one with all numbers positive was selected. The systems of polynomial, linear and differential equations were solved by Mappl6 software.

Drugs and chemicals

All common salts and reagents were AnalaR grade (Aldrich Chemicals). Adenosine 5′-triphosphate disodium salt (ATP), zinc chloride ($ZnCl_2$) and papain (crude powder) were purchased from Sigma/RBI (Deisenhofen, Germany).

Results

Zn^{2+} modulation of ATP-induced currents

All recorded TM neurons ($n = 59$) displayed responses to ATP, which were modulated by zinc in a reversible and concentration-dependent fashion. Application of zinc alone

(10–1000 μM) evoked no direct membrane response. The modulation of an ATP-induced current by Zn^{2+} was dependent on both the ATP- and the Zn^{2+} concentration (Figure 1); it exhibited a bell-shaped concentration–response curve. When P2X receptors were activated by 10 or 30 μM ATP, Zn^{2+} induced a potentiation at 3–30 μM (Figure 1a, top traces, d, f). The coapplication of 10 or 30 μM ATP plus 30 μM Zn^{2+} induced a maximal potentiation (up to 11- and 3.3-fold for 10 and 30 μM ATP, respectively). The Zn^{2+} EC_{50} for 10 μM ATP coapplication was 14 ± 1.3 μM ($n = 6$); for 30 μM ATP, the zinc EC_{50} was 5.4 ± 2.1 μM ($n = 3$). Higher Zn^{2+} concentrations (100–3000 μM) resulted in a decrease of the potentiation (Figure 1a, bottom traces, d, f). Note that the calculated maximal degree of the potentiation (Figure 1d, dashed lines) was about 30% higher than the envelope of the overlapping curve.

In contrast to the strong augmentation of responses to 10 and 30 μM ATP, Zn^{2+} elicited predominantly inhibitory effects on currents induced by 300 μM ATP (IC_{50} 178 ± 23 μM) (Figure 1d, f). The block produced by Zn^{2+} at 300 μM ATP was not complete even at 3 mM (65 ± 5%, Figure 1e, Table 1).

To correlate the modulating effect of zinc with the maximal amplitude of the ATP-induced current, 10 μM ATP + 30 μM zinc, 30 μM ATP + 30 μM zinc and 300 μM ATP + 10 μM zinc

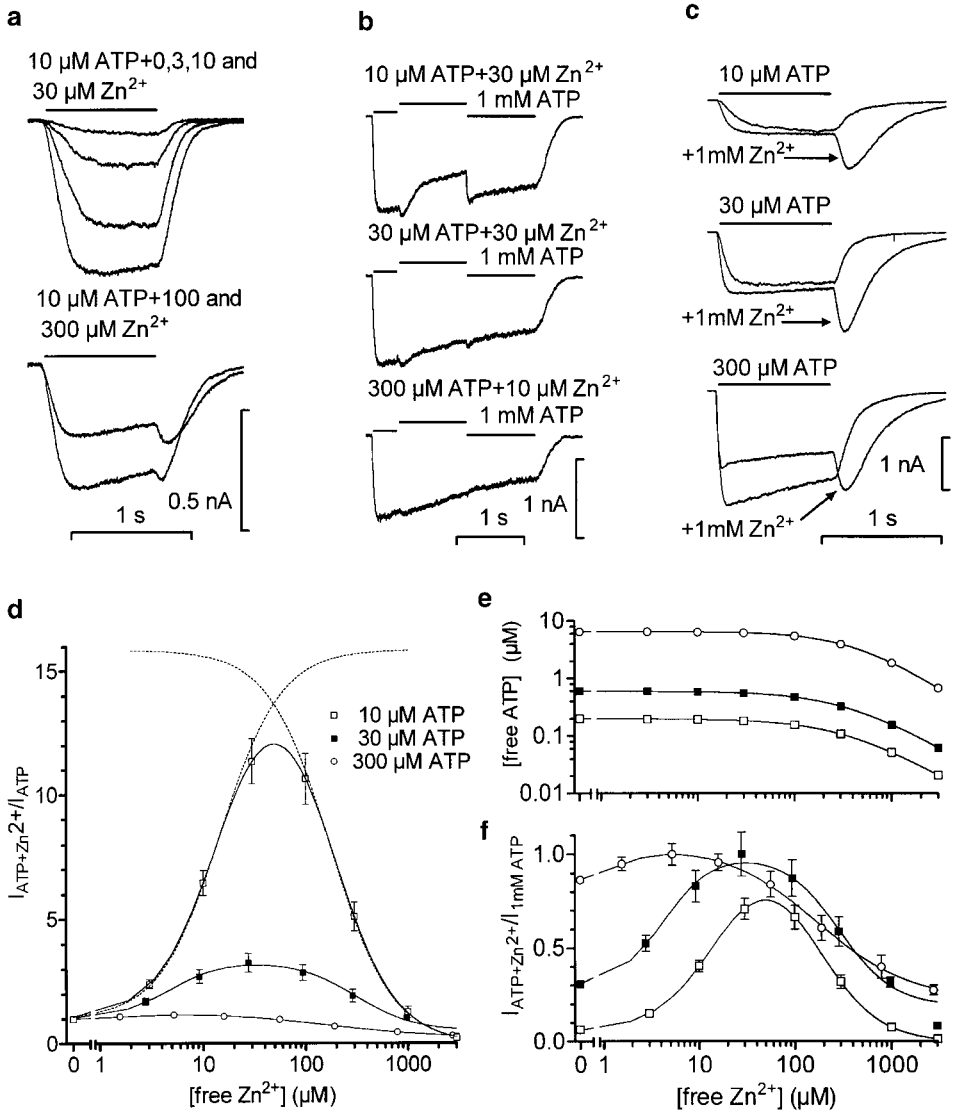

Figure 1 Modulation of ATP-induced currents by zinc. The current traces in (a–c) are from three different cells. (a) Whole-cell currents elicited by the 1 s application of 10 μM ATP alone and coapplication of 10 μM ATP with 3, 10, 30, 100 and 300 μM of zinc. (b) Comparison of currents to 1 mM ATP with the currents induced by coapplication of 10, 30, 300 μM ATP and zinc. Zinc was taken at concentrations eliciting a maximal potentiation of ATP-induced currents (10–30 μM). (c) Modulation of ATP (10, 30, 300 μM)-induced currents by 1 mM zinc. Note the tail currents after termination of zinc and ATP coapplication. The horizontal lines above current traces indicate duration of drug applications. (d) Analysis of concentration–response relation for zinc modulation of currents induced by 10, 30 and 300 μM ATP. Data are fitted by Equation (2). Dashed lines show deconvolution of the underlying potentiation (left bracket) and inhibition (right bracket) curves in Equation (2) taken separately after the fitting of the concentration–response relation for zinc at 10 μM ATP. (e) Calculated values for free ATP concentrations at 10, 30 and 300 μM of total ATP. (f) Analysis of the concentration–response relation identical to that in (d), but renormalized to the response to 1 mM ATP. For the fit with 300 μM ATP, the Hill slope for potentiation was fixed to 1.7.

Table 1 Zinc potentiation and inhibition of ATP currents

	Zinc potentiation				*Zinc inhibition*			
[Total ATP] (μM)	*EC_{50}* (μM)	*Hill coefficient*	*Maximum calculated potentiation (-fold)*	*Maximum observed potentiation (-fold)*	*IC_{50}* (μM)	*Hill coefficient*	*Unblocked part of current*	n
10	14±1.3	1.46±0.07	16±1	11±1	180±15	1.4±0.1	0±0.05	6
30	4.7±0.8	1.7±0.5	3.3±0.3	3.27±0.3	305±95	1.6±0.5	0.19±0.12	3
300	1.4±0.1	1.7 (fixed)	1.2±0.05	1.17±0.05	178±23	0.9±0.1	0.21±0.05	5

were applied immediately after 1 mM ATP (Figure 1b). Zinc was taken at a concentration inducing maximal augmentation of the corresponding ATP-activated current. The amplitude ratios of the zinc-modulated ATP responses to the 1 mM ATP-evoked responses were 0.7±0.03, 1.06±0.05 and 1±0.03 for responses induced by 10, 30 and 300 μM ATP + zinc, respectively ($n=5$ cells). These numbers were used to normalize the concentration–response relations for Zn^{2+} (Figure 1f). At any used ATP concentration, the maximal potentiation by zinc was limited by the maximal amplitude of the ATP-induced current. The minimal enhancement during coapplication of zinc and 300 μM ATP is due to the proximity of the response to 300 μM ATP to the maximal ATP response.

Comparison of concentration-response relations for zinc and the calculated decline of free ATP concentration (Figure 1e) suggest that at 10 and 30 μM ATP the last points in the graph may be affected by the decline of free ATP concentration. The reduction of free Zn^{2+} due to chelation is given in μM as a fraction [Zn^{2+}]/[total Zn] for some selected points: at 10 μM ATP, 0.97/1, 993/1000; at 30 μM ATP, 0.92/1, 94/100, 978/1000; at 300 μM ATP, 0.52/1, 5.2/10, 56/100, 190/300, 790/1000, 2733/3000. Calculations indicate that the decrease in Zn^{2+} concentration at 10 and 30 μM ATP is negligible, while the concentration response curve obtained at 300 μM ATP was rescaled for the concentration of free zinc (Figure 1d, f).

Effect of zinc on the concentration dependence of ATP-induced currents

The concentration–response relation for ATP was measured in two extracellular solutions: the standard containing 2.5 mM Ca^{2+} and 1.5 mM Mg^{2+} (Figure 2a) and the test solution containing 1.2 mM Ca^{2+} and 0 mM Mg^{2+} (Figure 2b). The ATP concentration–response relation depended on the concentrations of divalent metal ions (Figure 2c), $EC_{50}=48.8\pm1.5$ and 11 ± 0.2 μM, respectively, Hill coefficients for both fit 1.6 (equation (1)). However, when the data were replotted on the basis of the calculated values for free ATP rather than the total ATP concentration, the concentration–response plots for ATP in different extracellular solution were congruent within the limits of the error bars (Figure 2d); in standard solution the EC_{50} was 1 ± 0.04 μM, $h=1.6\pm0.08$, $n=7$, and in solution containing 1.2 mM Ca^{2+} and 0 mM Mg^{2+}, the EC_{50} was 1.1 ± 0.02 μM, $h=1.6\pm0.05$, $n=7$. To eliminate the effects of complex formation of divalent cations with ATP, the concentration–response curves for ATP in the presence of different zinc concentrations were also analyzed using the concentration of free ATP (Figure 2d). Zinc at 5 and 50 μM caused a leftward shift in the concentration–response curve without affecting the maximal response. At 5 and 50 μM, zinc reduced the EC_{50} to 0.32 ± 0.01 and 0.08 ± 0.003 μM of free ATP, respectively. Further increase in Zn^{2+} concentration to 1000 μM, weakly changed the apparent affinity of free ATP (EC_{50} 0.12 ± 0.01 μM), but strongly decreased its efficacy (the maximal response was reduced to 0.42 ± 0.01 of control response). An analysis considering the total ATP concentration yielded EC_{50}s for ATP in the presence of 5, 50 and 1000 μM Zn^{2+} of 15 ± 0.5, 4.8 ± 0.4 and 24.7 ± 1.5 μM, respectively.

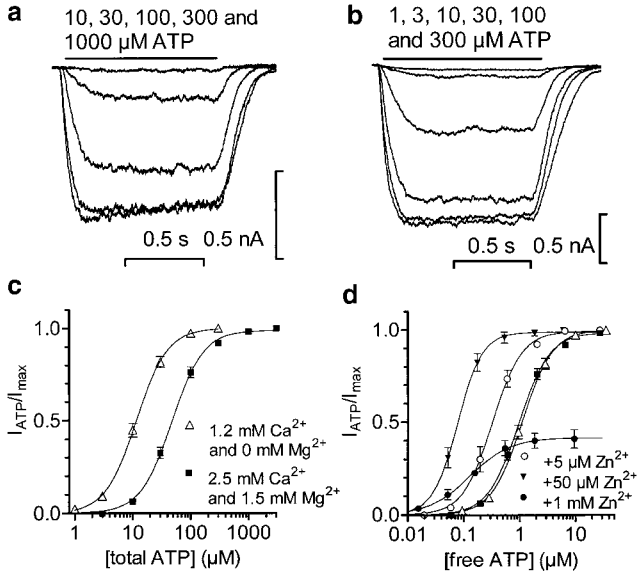

Figure 2 Concentration–respone relationships for ATP and ATP in the presence of zinc. (a) Whole-cell currents were evoked by ATP at the concentrations 10, 30, 100, 300 and 1000 μM; the outer (standard) solution contained 2.5 mM Ca^{2+} and 1.5 M Mg^{2+}. (b) Currents induced by ATP at 1, 3, 10, 30, 100 and 300 μM in another cell recorded with the outer solution containing 1.2 mM Ca^{2+} and 0 mM Mg^{2+}. (c) Concentration–response relationships for ATP in 1.2 mM Ca^{2+} and 0 mM Mg^{2+} and for ATP in 2.5 mM Ca^{2+}- and 1.5 mM Mg^{2+}-containing solution. The data are fitted with the Equation (1) with the following values: $EC_{50}=11.6\pm0.4$ μM, $h=1.6\pm0.05$ for the 0 Mg^{2+}-containing solution and $EC_{50}=48.8\pm1.5$ μM, $h=1.5\pm0.1$ for the standard solution. (d) Concentration–response relationships displayed against free ATP +5, 50, 1000 μM Zn^{2+} and those shown in (c) (same symbols in (c) and (d)). Data points are fitted by the Equation (1). The respective values for EC_{50} and Hill coefficients for the ATP-induced currents in the solutions containing: (i) 0 Mg^{2+}, 1.2 Ca^{2+}; (ii) 1.5 Mg^{2+}, 2.5 Ca^{2+}; (iii) 1.5 Mg^{2+}, 2.5 Ca^{2+} +5, 50 and 1000 μM Zn^{2+} are: (i) 1.1 ± 0.05 μM and 1.6 ± 0.04; (ii) 1 ± 0.06 μM and 1.6 ± 0.08; (iii) 0.4 ± 0.1 μM and 1.6 ± 0.1; 0.08 ± 0.002 μM and 1.9 ± 0.07; 0.12 ± 0.01 μM and 1.2 ± 0.07, respectively. All responses are normalized to the current elicited by 1 mM ATP. Numbers of cells were 7, 7, 4, 3, 4 in the same order. Zinc was coapplied with ATP for 1 s. The peak amplitudes of currents during the application are measured.

Zinc modulation of ATP-activated currents is voltage independent

To reveal possible channel-blocking effects of high zinc concentrations that could account for the noncompetitive zinc inhibition (see Figure 1d), we analyzed the current–voltage relation of ATP-induced currents in the absence and presence of 300 μM zinc. Zinc inhibited the current activated by 300 μM ATP at membrane voltages between -75 and $+40$ mV to the same extent and did not change the reversal potential of ATP responses (three cells).

Influence of zinc on the kinetics of ATP responses

Zinc increased the decay time of ATP-evoked currents (Figure 1a,c). To analyze this effect, we applied ATP in the presence of zinc. Figure 3a,c illustrates the influence of metal ions on the deactivation rate after ATP offset. The kinetics were examined in control conditions with 10 μM ATP and in the presence of 3, 10, 30, 100, 300 and 1000 μM zinc. In all experiments, the time course of deactivation could be well fitted with a single exponential function whose time constant (τ_{deact}) was used to quantify the kinetics of this process. Zinc slowed the deactivation process in a concentration-dependent manner (Figure 3c). The τ_{deact} increased from 55 ± 6 ms in the absence of zinc to 512 ± 12 ms at 1 mM zinc ($n=5$), or by a factor of about 9, providing an EC_{50} value of 63 ± 4 μM zinc with a Hill slope of 1.3 ± 0.1.

To measure the rate of Zn^{2+} dissociation, the metal ion was applied during a steady-state ATP (30 μM) response, so that the onset and reversal of the effects of Zn^{2+} could be observed during a single agonist response. Figure 3b shows augmentation of ATP current by 10 μM Zn^{2+} (upper trace) and a reversal of the potentiation with the time constant of 190 ms. At 100 μM, Zn^{2+} concentration was increased up to 100 μM, the potentiation was still observed, but it was impeded by a slowly developing inhibition (Figure 3b, middle trace). When zinc was washed out, the ATP-induced current transiently increased ('tail current') and then recovered gradually to the control level. At 1 mM, Zn^{2+} induced only a marginal potentiation of ATP current, but upon removal of zinc, there was a rapid increase of the current followed by a slow decline towards the response amplitude seen with ATP alone (Figure 3b, bottom trace). A similar tail current was also observed after simultaneous washout of ATP and zinc (Figure 1a, lower panel, c). The decay time of the zinc effect was about the same at all tested concentrations (200–300 ms).

Kinetic modeling of the transient currents at zinc and ATP removal

There are several possible kinetic alterations that could lead to a slowing of current deactivation and appearance of the tail current. We developed a model aimed at demonstrating that the tail current following washout of zinc and ATP is compatible with an allosteric mechanism of the Zn^{2+}-induced block and reflects a change in the balance between the potentiating and inhibitory effects of zinc, caused by the rapid dilution of substances.

Figure 4a presents the receptor states, which are directly associated with channel openings. At equilibrium, in the presence of 1 mM Zn^{2+} and 30 μM ATP (0.5 μM of free ATP),

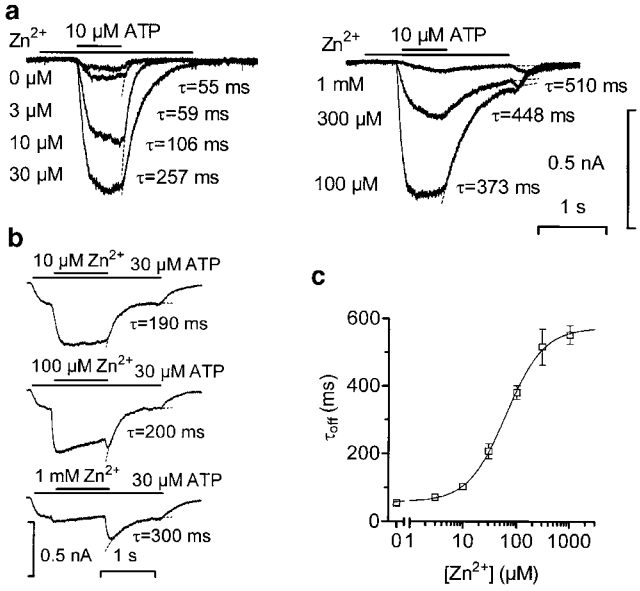

Figure 3 Kinetic features of zinc modulation of ATP-induced currents. (a) Whole-cell currents induced by 600 ms perfusion of 10 μM ATP and 10 μM ATP in the continuous presence of 3, 10, 30, 100, 300 and 1000 μM of zinc. Zinc was applied 600 ms before ATP and washed out 1 s after the end of ATP application. The deactivation time (τ_{off}) was measured by single exponential fitting of current decay after ATP withdrawal. All recordings are from a single cell. (b) Another cell. Zinc recovery kinetics in the presence of ATP. Zinc was applied at 10, 100 and 1000 μM for 1 s in the presence of 30 μM ATP. The current decay is fitted by a single exponential. (c) Dependence of the deactivation time of ATP-induced currents on the zinc concentration. Data are taken from experiments similar to those presented in Figure 4a. Data were fitted with a logistic equation with the following parameters: τ_{off} for ATP response alone 59 ± 6 ms, $EC_{50}=63\pm4$ μM, $n=1.3\pm0.1$ and τ_{off} max $=512\pm12$ ms, $n=5$ cells.

most of the receptors are in the state RZAB because the concentrations of both substances exceed the corresponding EC_{50} values for Zn^{2+}-induced potentiation and inhibition. The agonist molecule is bound, but the transitions to the open state are suppressed because the blocking site is occupied too. After withdrawal of both ATP and Zn^{2+}, there are two ways for the receptor to lose the agonist molecule. First, ATP can unbind from the receptor directly ($\tau_{off}=550$ ms). Second, the receptor makes two transitions: (1) The blocking molecule unbinds (τ_{off} about 30 ms) and the receptor passes to the state RZA where the channel openings are more probable and the receptor-mediated current increases. (2) The agonist dissociates from the receptor. When the ATP current decays in 10 the presence of zinc (Figure 3a), the channel openings are five-fold reduced and the time that the receptor spends in the open state is negligible. The probability of open state for the P2X2 receptor in control conditions is about 0.5 ($P_0=0.6$, Ding & Sachs, 1999), and since the agonist can unbind only from the closed state of the receptor, the current will decay for about 1 s.

The second model (Figure 4c) does not differ conceptually from the first one, but includes the dissociation of zinc from the binding site responsible for potentiation of the P2X receptor. Zinc unbinds from the receptor with a time constant of 200 ms and the receptor enters into the states RAB or RA. From these states, the ATP molecule unbinds much faster. However, the situation does not change in principle, and the conditions for appearance of the tail current persist. The

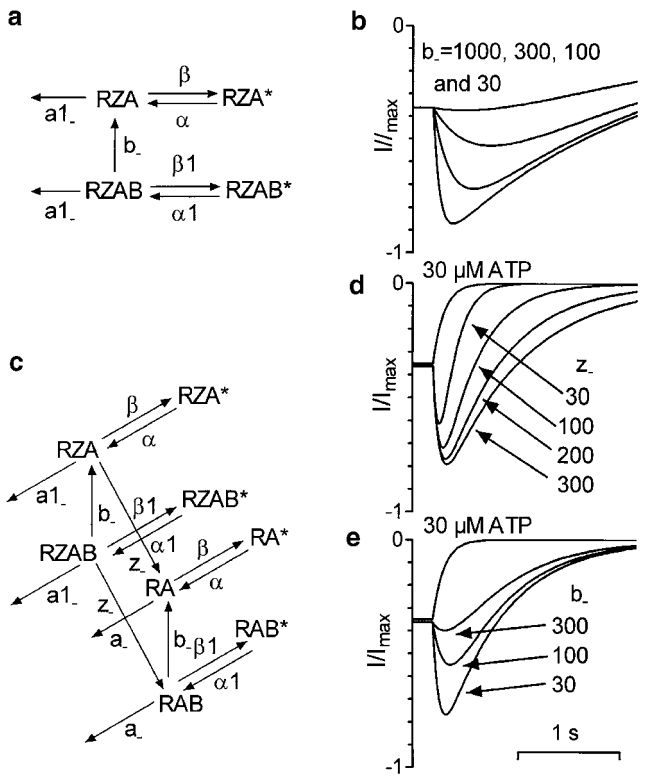

Figure 4 Proposed kinetic schemes for the tail current at removal of zinc and ATP from the P2X receptor. (a) Four-state model. The shown states of receptor are: RZA, receptor occupied by Zn^{2+} at potentiating site (Z) and by agonist molecule (A). In this state, the receptor can bind zinc at another site causing the transition of the receptor to the blocked state RZAB. From both states, the receptor can enter the open states RZA* or RZAB*. However, transitions between RZAB and RZAB* result in a lower open-state probability. The scheme shows the transitions after removal of agonist and blocker molecules. (b) Simulation of current traces after removal of ATP and zinc. The current traces were generated with $b_- = 1000$, 300, 100, 30 using scheme (a). (c) Eight-state model. The same as above, but four receptor states with Zn^{2+} unbound from its sites on the ATP receptor are added: RA, RAB, RA* and RAB*. (d) Simulation of current traces using the scheme (c) with $z_- = 30$, 100, 200 and 300. (e) Simulation of current traces using the scheme (c) with $b_- = 30$, 100 and 300. At the first step the schemes were considered closed. The system of linear equations was solved to find the equilibrium for receptor states inside it. Then the differential equations were solved. Unless otherwise specified, the rate constants were set to: $\beta = \alpha = 1000$ ($P_0 = 0.6$; Ding & Sachs, 1999), $\beta 1 = \beta/3.3$, $\alpha 1 = \alpha^*3.3$ (the coefficient is adjusted to 3.3 to block the ATP-induced current by 80%, Figure 1f), $a1_- = 1/0.55$ ($1/\tau_{deact}$ Figure 3c, maximal value), $b_- = 1/0.03$ (1/onset of tail current, Figure 1c), $b_+ = 1000^*30/178$ ($[Zn^{2+}]^*b_-/IC_{50}$, Figure 1d), $z_- = 1/0.2$ ($1/\tau_{deact}$ for Zn^{2+}-induced potentiation, Figure 3b), $z_+ = 1000^*5/14$ ($[Zn^{2+}]^*z_-/EC_{50}$), $a_- = 1/(0.06/2)$ ($1/\tau_{deact}/2$, Figure 3c, half of the minimal value). Dimensions: s^{-1} and μM^{-1}.

simulated parameters of the tail current coincide well with those observed in our experiments. Figure 4d, e also demonstrates that the simulated tail currents are the result of ATP–Zn^{2+} interaction through a wide range of kinetic parameters.

Discussion and conclusions

Zinc exerts a potent biphasic modulation of native P2X receptors in TM neurons. The extent of potentiation or inhibition by zinc depends on both the metal ion concentration and the concentration of ATP used to elicit the response. Such a bidirectional modulation of P2X receptor-mediated responses by zinc has been demonstrated in superior cervical ganglion neurons (Cloues *et al*., 1993), in preganglionic vagal neurons (Ueno *et al*., 2001) and recombinant $P2X_2$, $P2X_3$, $P2X_4$ and $P2X_{2/6}$ receptors expressed in *Xenopus* oocytes (Seguela *et al*., 1996; Soto *et al*., 1996; Wildman *et al*., 1998; Acuna-Castillo *et al*., 2000; King *et al*., 2000). The Zn^{2+} concentrations for potentiation and suppression of P2X receptor-mediated responses in these studies are very close to those in our study.

Concentration–response analysis was performed using free ATP concentration in extracellular solution. It shows that 5–50 μM zinc shifted the concentration-response relation for ATP to the left and did not affect the maximal amplitude of ATP-induced current, suggesting that zinc potentiated the agonist response by allosterically enhancing the affinity of agonist binding. Further increase of the zinc concentration up to 1 mM does not change the EC_{50} for ATP dramatically, but halves the maximal amplitude. The moderate decrease in the rise of ATP affinity in the presence of 1 mM zinc may be due to an allosteric character of the inhibition. During such a block, the fraction of receptors in the active state decreases, and because the agonist can leave the receptor only from the closed state, the agonist unbinds faster, resulting in a decrease of the apparent affinity. The probability of the open state of $P2X_2$ receptors ($P_0 = 0.6$; Ding & Sachs, 1999; Whitlock *et al*., 2001) suggests dependence of the apparent affinity on channel gating (Colquhoun, 1998).

These observations correlate well with the biphasic dose–response relation for zinc at a fixed ATP concentration, where zinc first enhanced ATP-induced current with an EC_{50} of 14 μM and then suppressed it at higher zinc concentrations. The effect of zinc was greatest at lower concentrations of ATP, which activated only a small fraction of the maximal current. The zinc-induced potentiation was evident at 10–30 μM ATP, but weak at 300 μM ATP. There was a remarkable difference in the suppression of ATP currents by high zinc concentrations at different ATP concentrations. Inhibition of the ATP current at 300 μM ATP was clearly not complete. The full decline of currents at 10 μM ATP is consistent with depletion of free ATP. The concentration–response relation for Zn^{2+} at 30 μM ATP follows the relation obtained at 300 μM ATP until 1 mM Zn^{2+}, but the last point at 3 mM Zn^{2+} does not follow the fit (Figure 1f). In this case, Zn^{2+} inhibits the current, which is maximally potentiated by a lower Zn^{2+} concentration until ATP chelation achieves a critical value (Figure 1e).

At low concentrations up to 50 μM, zinc increased both the ATP affinity and the time constant of the ATP off-relaxation, τ_{off}. The simplest explanation for this observation is a slowing of the ATP dissociation from its binding site. There is some discrepancy between the Zn^{2+} concentration–deactivation time and concentration–response relations. The deactivation time rises through the whole range of Zn^{2+} concentrations, while the EC_{50} has its minimum at 50 μM Zn^{2+}. This mismatch could be explained in several ways. As noted above, the suppression of channel gating halves the apparent affinity with $P_0 = 0.6$. With regard to the doubled deactivation time at 50–1000 μM Zn^{2+}, this may only compensate for the corresponding increase of apparent affinity. However, the probability for the open state was obtained for excised patches and may not

exactly fit our case. If P_0 were about 0.8 or 0.9, the expected increase in EC_{50} would be three- or five-fold, respectively and would overcome the increase of the affinity related with the rising deactivation time. In addition to slowing the ATP dissociation, zinc may affect its association as well. The decrease of apparent affinity of the binding site for ATP by zinc was reported for dorsal root ganglion neurons (Li *et al*., 1997).

Our results are consistent with the existence of two distinct zinc modulatory sites on the P2X receptor. The high-affinity modulatory site for zinc appears to be associated with a potentiation of the ionophore function, distinct from the low-affinity inhibitory site. Two distinct binding sites with different affinities and mechanisms have been proposed by Ueno *et al*. (2001). Experimental support for this interpretation is provided by the different apparent binding affinities of zinc potentiation and inhibition, as well as by the influence of zinc on the offset kinetics of the ATP-mediated current. While there is a consensus that zinc potentiates P2X2 receptors allosterically (Wildman *et al*., 1998; Xiong *et al*., 1999), and our experiments specify the parameters of this effect for TM neurons, the nature of zinc-induced inhibition remains uncertain. There are several mechanisms by which zinc can produce receptor inhibition. These include (1) open channel block, (2) allosteric inhibition and (3) acceleration of desensitization. The latter is unlikely, as we did not observe a change in the rate of ATP response desensitization at any zinc concentration. During the open channel block, the channel cannot close while blocked, resulting in the prolongation of deactivation time. This would explain the appearance of the tail currents after substance removal. However, our modeling features the tail currents as an essential attribute of responses to ATP + Zn^{2+} during allosteric block. Furthermore, should the open channel block increase the probability of the open state, this would result in an increase of the apparent agonist affinity. But as we have shown, this is not the case. The observation that the Zn^{2+}-induced inhibition is incomplete and voltage-independent also supports an allosteric mechanism of zinc action. Our data suggest that the effects of inhibitory concentrations of zinc are a consequence of blocking the gating rather than the open channel or the ion permeability ratio.

The existence of multiple binding sites for zinc and different localization of positive and negative modulatory sites at P2X receptors are further supported by a recent mutation study (Clyne *et al*., 2002) using site-directed mutagenesis. Of the seven cloned P2X subunits $P2X_2$, $P2X_4$ and $P2X_6$ mRNA transcripts and proteins were determined in TM (Collo *et al*., 1996; Loesch & Burnstock, 2001). Our pharmacological and scPCR data suggest that P2X receptors expressed functionally in TM neurons seem to be characterized by $P2X_2$ homomeric receptor (Vorobjev *et al*., 2003). Extracellular zinc reaches concentrations in the high micromolar range during neuronal activity (Assaf & Chung, 1984; Howell *et al*., 1984; Anikszteljn *et al*., 1987) and may thus physiologically regulate ATP–P2x–receptor interactions in the hypothalamus.

Supported by Deutsche Forschungsgemeinschaft HA 1525/6-4 and a Lise-Meitner-Stipend to O.A.S.

References

ACUNA-CASTILLO, C., MORALES, B. & HUIDOBRO-TORO, J.P. (2000). Zinc and copper modulate differentially the P2X4 receptor. *J. Neurochem.,* **74,** 1529–1537.

ANIKSZTEJN, L., CHARTON, G. & BEN ARI, Y. (1987). Selective release of endogenous zinc from the hippocampal mossy fibers *in situ*. *Brain Res.,* **404,** 58–64.

ASSAF, S.Y. & CHUNG, S.H. (1984). Release of endogenous Zn^{2+} from brain tissue during activity. *Nature,* **308,** 734–736.

BRAKE, A.J. & JULIUS, D. (1996). Signaling by extracellular nucleotides. *Annu. Rev. Cell Dev. Biol.,* **12,** 519–541.

CLOUES, R., JONES, S. & BROWN, D.A. (1993). Zn^{2+} potentiates ATP-activated currents in rat sympathetic neurons. *Pflugers Arch.,* **424,** 152–158.

CLYNE, J.D., LAPOINTE, L.D. & HUME, R.I. (2002). The role of histidine residues in modulation of the rat P2X(2) purinoceptor by zinc and pH. *J. Physiol.,* **539,** 347–359.

COLLO, G., NORTH, R.A., KAWASHIMA, E., MERLO-PICH, E., NEIDHART, S., SURPRENANT, A. & BUELL, G. (1996). Cloning of P2X5 and P2X6 receptors and the distribution and properties of an extended family of ATP-gated ion channels. *J. Neurosci.,* **16,** 2495–2507.

COLQUHOUN, D. (1998). Binding, gating, affinity and efficacy: the interpretation of structure – activity relationships for agonists and of the effects of mutating receptors. *Br. J. Pharmacol.,* **125,** 924–947.

DING, S. & SACHS, F. (1999). Single channel properties of P2X2 purinoceptors. *J. Gen. Physiol.,* **113,** 695–720.

EDWARDS, F.A., GIBB, A.J. & COLQUHOUN, D. (1992). ATP receptor-mediated synaptic currents in the central nervous system. *Nature,* **359,** 144–147.

EVANS, R.J., DERKACH, V. & SURPRENANT, A. (1992). ATP mediates fast synaptic transmission in mammalian neurons. *Nature,* **357,** 503–505.

EVANS, R.J., LEWIS, C., VIRGINIO, C., LUNDSTROM, K., BUELL, G., SURPRENANT, A. & NORTH, R.A. (1996). Ionic permeability of, and divalent cation effects on, two ATP-gated cation channels (P2X receptors) expressed in mammalian cells. *J. Physiol.,* **497,** 413–422.

FREDERICKSON, C.J. & BUSH, A.I. (2001). Synaptically released zinc: physiological functions and pathological effects. *Biometals,* **14,** 353–366.

FURUKAWA, K., ISHIBASHI, H. & AKAIKE, N. (1994). ATP-induced inward current in neurons freshly dissociated from the tuberomammillary nucleus. *J. Neurophysiol.,* **71,** 868–873.

GALLIGAN, J.J. & BERTRAND, P.P. (1994). ATP mediates fast synaptic potentials in enteric neurons. *J. Neurosci.,* **14,** 7563–7571.

HOWELL, G.A., WELCH, M.G. & FREDERICKSON, C.J. (1984). Stimulation-induced uptake and release of zinc in hippocampal slices. *Nature,* **308,** 736–738.

KANJHAN, R., HOUSLEY, G.D., BURTON, L.D., CHRISTIE, D.L., KIPPENBERGER, A., THORNE, P.R., LUO, L. & RYAN, A.F. (1999). Distribution of the $P2X_2$ receptor subunit of the ATP-gated ion channels in the rat central nervous system. *J. Comp. Neurol.,* **407,** 11–32.

KHAKH, B.S. (2001). Molecular physiology of P2X receptors and ATP signalling at synapses. *Nat. Rev. Neurosci.,* **2,** 165–174.

KING, B.F., TOWNSEND-NICHOLSON, A., WILDMAN, S.S., THOMAS, T., SPYER, K.M. & BURNSTOCK, G. (2000). Coexpression of rat P2X2 and P2X6 subunits in Xenopus oocytes. *J. Neurosci.,* **20,** 4871–4877.

KOSHIMIZU, T.A., Van GOOR, F., TOMIC, M., WONG, A.O., TANOUE, A., TSUJIMOTO, G. & STOJILKOVIC, S.S. (2000). Characterization of calcium signaling by purinergic receptor-channels expressed in excitable cells. *Mol. Pharmacol.,* **58,** 936–945.

LI, C., PEOPLES, R.W. & WEIGHT, F.F. (1997). Inhibition of ATP-activated current by zinc in dorsal root ganglion neurones of bullfrog. *J. Physiol.,* **505** (Part 3), 641–653.

LOESCH, A. & BURNSTOCK, G. (2001). Immunoreactivity to P2X(6) receptors in the rat hypothalamo-neurohypophysial system: an ultrastructural study with extravidin and colloidal gold-silver labelling. *Neuroscience,* **106,** 621–631.

NAKAZAWA, K., LIU, M., INOUE, K. & OHNO, Y. (1997). Potent inhibition by trivalent cations of ATP-gated channels. *Eur. J. Pharmacol.,* **325,** 237–243.

NORENBERG, W. & ILLES, P. (2000). Neuronal P2X receptors: localisation and functional properties. *Naunyn Schmiedeberg's Arch. Pharmacol.,* **362,** 324–339.

NORTH, R.A. & SURPRENANT, A. (2000). Pharmacology of cloned P2X receptors. *Annu. Rev. Pharmacol. Toxicol.,* **40,** 563–580.

RALEVIC, V. & BURNSTOCK, G. (1998). Receptors for purines and pyrimidines. *Pharmacol. Rev.,* **50,** 413–492.

SEGUELA, P., HAGHIGHI, A., SOGHOMONIAN, J.J. & COOPER, E. (1996). A novel neuronal P2x ATP receptor ion channel with widespread distribution in the brain. *J. Neurosci.,* **16,** 448–455.

SHARONOVA, I.N., VOROBJEV, V.S. & HAAS, H.L. (2000). Interaction between copper and zinc at GABA(A) receptors in acutely isolated cerebellar Purkinje cells of the rat. *Br. J. Pharmacol.,* **130,** 851–856.

SIGEL, H. (1987). Isomeric equilibria in complexes of adenosine 5′-triphosphate with divalent metal ions. Solution structures of M(ATP)2-complexes. *Eur. J. Biochem.,* **165,** 65–72.

SMART, T.G., XIE, X. & KRISHEK, B.J. (1994). Modulation of inhibitory and excitatory amino acid receptor ion channels by zinc. *Prog. Neurobiol.,* **42,** 393–341.

SORIMACHI, M., ISHIBASHI, H., MORITOYO, T. & AKAIKE, N. (2001). Excitatory effect of ATP on acutely dissociated ventromedial hypothalamic neurons of the rat. *Neuroscience,* **105,** 393–401.

SOTO, F., GARCIA-GUZMAN, M., GOMEZ-HERNANDEZ, J.M., HOLLMANN, M., KARSCHIN, C. & STUHMER, W. (1996). P2X4: an ATP-activated ionotropic receptor cloned from rat brain. *Proc. Natl. Acad. Sci. U.S.A.,* **93,** 3684–3688.

UENO, T., UENO, S., KAKAZU, Y., AKAIKE, N. & NABEKURA, J. (2001). Bidirectional modulation of P2X receptor-mediated response by divalent cations in rat dorsal motor nucleus of the vagus neurons. *J. Neurochem.,* **78,** 1009–1018.

VIRGINIO, C., CHURCH, D., NORTH, R.A. & SURPRENANT, A. (1997). Effects of divalent cations, protons and calmidazolium at the rat P2X7 receptor. *Neuropharmacology,* **36,** 1285–1294.

VOROBJEV, V.S., SHARONOVA, I.N. & HAAS, H.L. (1996). A simple perfusion system for patch-clamp studies. *J. Neurosci. Methods,* **68,** 303–307.

VOROBJEV, V.S., SHARONOVA, I.N., HAAS, H.L. & SERGEEVA, O.A. (2003). Expression and function of p2X purinoceptors in rat histaminergic neurons. *Br. J. Pharmacol.,* **138,** 1013–1019.

WHITLOCK, A., BURNSTOCK, G. & GIBB, A.J. (2001). The single-channel properties of purinergic P2X ATP receptors in outside-out patches from rat hypothalamic paraventricular parvocells. *Pflugers Arch.,* **443,** 115–122.

WILDMAN, S.S., BROWN, S.G., RAHMAN, M., NOEL, C.A., CHURCHILL, L., BURNSTOCK, G., UNWIN, R.J. & KING, B.F. (2002). Sensitization by extracellular Ca(2+) of rat P2X(5) receptor and its pharmacological properties compared with rat P2X(1). *Mol. Pharmacol.,* **62,** 957–966.

WILDMAN, S.S., KING, B.F. & BURNSTOCK, G. (1998). Zn^{2+} modulation of ATP-responses at recombinant P2X2 receptors and its dependence on extracellular pH. *Br. J. Pharmacol.,* **123,** 1214–1220.

XIANG, Z., BO, X., OGLESBY, I., FORD, A. & BURNSTOCK, G. (1998). Localization of ATP-gated P2X2 receptor immunoreactivity in the rat hypothalamus. *Brain Res.,* **813,** 390–397.

XIONG, K., PEOPLES, R.W., MONTGOMERY, J.P., CHIANG, Y., STEWART, R.R., WEIGHT, F.F. & LI, C. (1999). Differential modulation by copper and zinc of P2X2 and P2X4 receptor function. *J. Neurophysiol.,* **81,** 2088–2094.

(Received December 24, 2002
Revised March 19, 2003
Accepted April 9, 2003)